Si(100)2×3-Na surface phase: Formation and atomic arrangement

A. A. Saranin

Department of Electronic Engineering, Faculty of Engineering, Osaka University, Suita, Osaka 565, Japan;
Institute of Automation and Control Processes, 690041 Vladivostok, Russia;
and Faculty of Physics and Engineering, Far Eastern State University, 690000 Vladivostok, Russia

A. V. Zotov

Department of Electronic Engineering, Faculty of Engineering, Osaka University, Suita, Osaka 565, Japan;
Department of Electronics, Vladivostok State University of Economics and Service, 690600 Vladivostok, Russia;
and Institute of Automation and Control Processes, 690041 Vladivostok, Russia

S. V. Ryzhkov, D. A. Tsukanov, and V. G. Lifshits

Institute of Automation and Control Processes, 690041 Vladivostok, Russia

J.-T. Ryu, O. Kubo, H. Tani, T. Harada, M. Katayama, and K. Oura*

Department of Electronic Engineering, Faculty of Engineering, Osaka University, Suita, Osaka 565, Japan

(Received 22 December 1997)

Using scanning tunneling microscopy (STM), we have studied the formation and structure of the Si(100)2×3-Na surface phase. It has been found that both the formation process and atomic arrangement of the Si(100)2×3-Na surface differ substantially from those known for 2×3 reconstructions induced by other alkali and alkaline earth metals, since the Si(100)2×3-Na phase is the only one in which the top Si layer undergoes a substantial reordering. The Si-atom density in the Si(100)2×3-Na surface phase has been determined to be 1/3 ML. A structural model of the Si(100)2×3-Na reconstruction has been proposed, and its registry to STM images has been discussed. [S0163-1829(98)01131-X]

I. INTRODUCTION

A great variety of ordered structures has been observed during deposition of submonolayer metal films on silicon crystalline surfaces.[1] Among those structures, there are several that are common for a number of different adsorbates. However, similar periodicity does not necessarily imply a similar atomic arrangement. The Si(111)$\sqrt{3}\times\sqrt{3}$ reconstruction furnishes an illustrative example of such a structure. Several types of Si(111)$\sqrt{3}\times\sqrt{3}$ structure are known: the $\sqrt{3}\times\sqrt{3}$ reconstruction induced by group-III atoms (Al, Ga, In) is formed by adatoms occupying T_4 sites on a bulklike terminated Si(111) surface,[2–4] boron atoms in the $\sqrt{3}\times\sqrt{3}$-B phase occupy S_5 substitutional sites directly beneath Si adatoms,[5] $\sqrt{3}\times\sqrt{3}$-Sb and $\sqrt{3}\times\sqrt{3}$-Bi structures are built of adsorbate trimers,[6–8] the $\sqrt{3}\times\sqrt{3}$-Ag phase has a complicated honeycomb chained trimer structure,[9] etc.

Another example of a common structure is Si(111)3×1 reconstruction induced by alkali metals such as Li, Na, K, and Cs.[10–13] The structure of Si(111)3×1 surfaces has been a subject of furious debates which still seem to be far from providing a conclusive consensus.[12–18] However, it is now commonly supposed that the atomic structure of the Si(111)3×1 reconstruction should be very similar for all metals, and is predominantly a Si(111) substrate reconstruction.

It is particularly remarkable that the same alkali metals (except for Li, but also including the alkaline earth metals Ba and Sr), being adsorbed on a Si(100) surface, again form a common superstructure, namely, a Si(100)2×3 one.[19–30] In the structural models proposed for Si(100)2×3 reconstructions induced by K,[20] Cs,[23,24] Ba,[26] and Sr,[29] adsorbate atoms are assumed to reside on the *intact* the Si(100)2×1 substrate surface. However, for the case of Si(100)2×3-Na surface, Glander and Webb[22] suggested, from low-energy electron-diffraction (LEED) observations, that Na induces structural changes in the underlying Si. Thus the questions ''Is the atomic structure of Si(100)2×3 reconstruction similar for all metals?'' and ''Does Si-atom reordering take place at Si(100)2×3 surface phase formation?'' remain open.

In the present paper, we report results of a scanning tunneling microscopy (STM) study of Si(100)2×3-Na phase formation. Direct evidence has been found for Si-atom reordering, and top Si-atom density in the Si(100)2×3-Na surface phase has been determined. The obtained results allow us to propose a plausible model of the Si(100)2×3-Na structure.

II. EXPERIMENT

Experiments were carried out in an ultrahigh-vacuum chamber with a base pressure of 1.1×10^{-8} Pa equipped with STM (''Omicron'') and LEED systems. The substrates used were Sb-doped $0.05-\Omega$ cm Si(100) wafers. Atomically clean Si(100) surfaces were prepared *in situ* by heating to 1250 °C after the samples were first outgassed at 600 °C for several hours. After this treatment, a sharp 2×1 LEED pattern was observed, and STM images corresponded to a well-ordered Si(100)2×1 surface. Sodium was deposited from a

thermal cell from SAES Getters Inc. The deposited Na coverage was estimated from a surface area covered by the Si(100)2×3-Na phase in STM images, assuming the saturation coverage of the 2×3-Na phase to be 1/3 ML in accordance with the data of Ref. 22. For STM observations, electrochemically etched tungsten tips cleaned by *in situ* heating were employed. All STM images presented in this paper were acquired at positive tip bias voltages (filled states). We were unable to acquire empty-state images in agreement with the prediction of theoretical work,[31] where an electrical field was shown to inhibit empty-state STM imaging of alkali metals on the Si(100) surface.

III. RESULTS AND DISCUSSION

Figure 1 demonstrates the evolution of surface structure during adsorption of Na on a Si(100)2×1 substrate held at about 400 °C. Figure 1(a) shows a filled-state STM image of a fresh Si(100)2×1 surface prior to Na deposition. The surface consists of flat terraces about 500 Å in width separated by monoatomic steps, and contains a modest number of surface defects. Na adsorption already alters the surface structure drastically at the very initial stages of Na deposition. As one can see in Fig. 1(b), the main features of this surface are the appearance of regions of 2×3 reconstruction near the step edges, and the formation of numerous furrows and islands on the terraces. Closer inspection reveals that the surface, both in the furrows and on top of the islands is covered by a 2×3 reconstruction (see Fig. 2). The direction of $3a$ periodicity on the 2×3 islands appears to be parallel to the direction of Si dimers of the original Si(100)2×1 surface. The 2×3 domains in the furrows are in the orthogonal orientation.

Such a behavior definitely indicates a significant Si mass transport during Si(100)2×3-Na surface phase formation. This means, in turn, that the top Si-atom density in the 2×3-Na phase should differ from 1 ML, the top Si-atom density of the original Si(100)2×1 surface. As a result, during 2×3-Na phase formation, excessive Si atoms are removed from the top Si monolayer in the regions which show up in STM images as furrows on Si(100)2×1 terraces. The released Si atoms agglomerate with each other and with arriving Na atoms, to form 2×3-Na islands. This process is shown schematically in Fig. 3(b).

Figure 3(b) also illustrates the growth of the 2×3-Na phase near the step edges. In this case, Si atoms detached from the step edge contribute to the spreading-out of the 2×3-Na phase over the lower terrace. Detachment of Si atoms from the step edge is believed to be a more likely process compared to extraction of Si atoms from their sites on the flat terrace. Thus, in the initial stages of 2×3-Na growth, the most extended areas of 2×3 reconstruction are observed near the step edges [see Fig. 1(b)]. The supply of Si atoms from a step edge continues until the step motion is blocked by a 2×3-Na island or a 2×3-Na furrow already formed on the upper terrace.

The process of 2×3-Na phase formation comes into saturation when no bare Si(100)2×1 regions are left, and the whole surface becomes covered by the Si(100)2×3-Na surface phase [Fig. 3(c)]. The STM image of such a surface is shown in Fig. 1(c). The surface contains 2×3-reconstructed
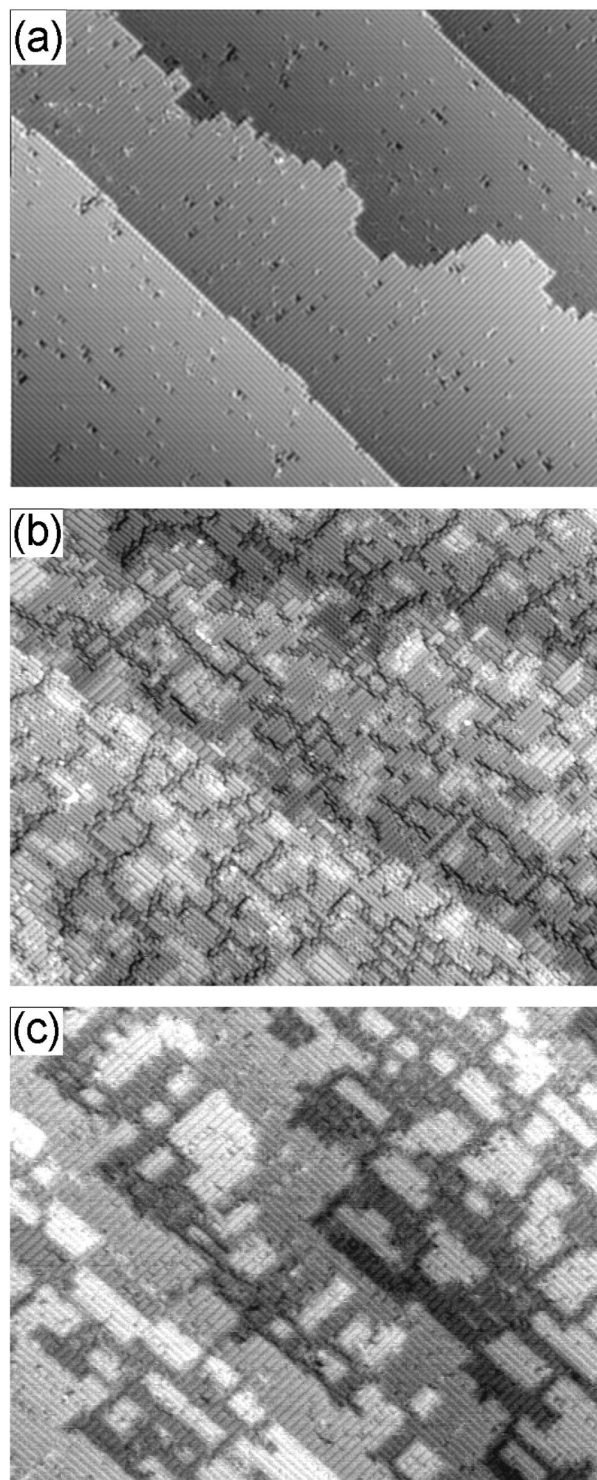

FIG. 1. Filled-state (+1.8 V, 0.2 nA) 1000×800-Å^2 STM images of Si(100)2×1 surface: (a) prior to Na deposition; (b) after deposition of about 0.15-ML Na; (c) after deposition of about 0.35-ML Na.

islands of basically rectangular shape. The area between islands also has a 2×3 reconstruction, but in the orthogonal orientation. The latter regions originate from the spreading out of the furrows observed at the early stages of Na adsorption. 2×3 regions on the upper terraces near the step edges are free of island as a result of the growth supplied by Si mass transport from the step edges.
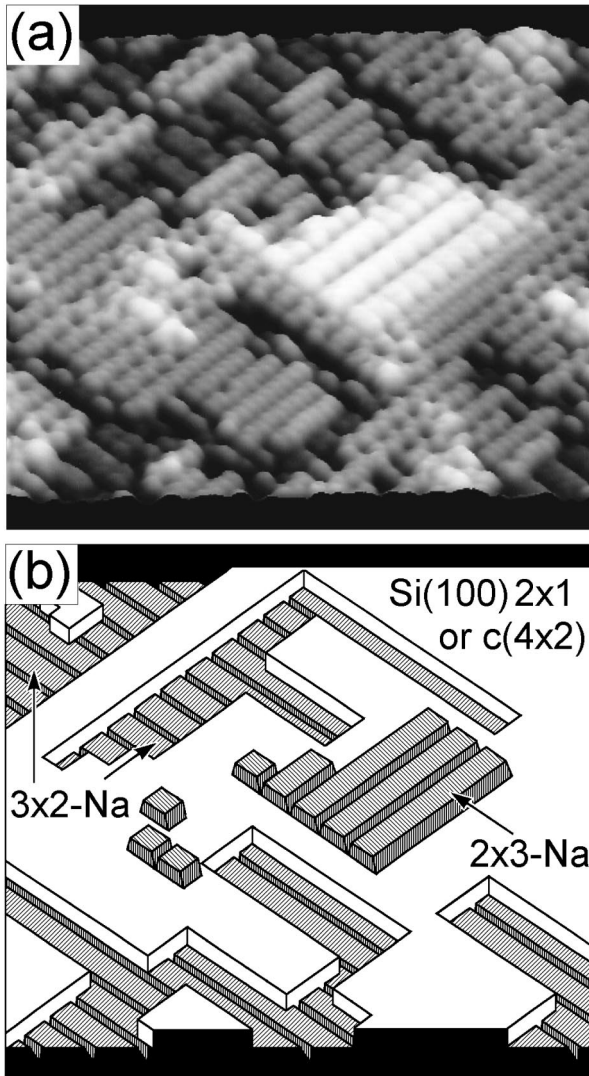
FIG. 2. (a) 3D STM presentation of 220×220-Å^2 area on Si(100) surface at the initial stage of Si(100)2×3-Na surface phase formation. (b) Schematic sketch of the shown area.

Determination of a fraction of the surface area covered by 2×3-Na islands (S) allows one to estimate the Si-atom density (Θ_{Si}) in the Si(100)2×3-Na surface phase. The surface between islands which occupies an area fraction of $1 - S$ is a source of Si atoms for 2×3-Na island formation, and it supplies $(1 - S)(1 - \Theta_{Si})$ (ML) of Si. This Si amount is accumulated in 2×3-Na islands and, thus, equals $S\Theta_{Si}$. Equating these values,

$$(1 - S)(1 - \Theta_{Si}) = S\Theta_{Si},$$

one can easily obtain that

$$\Theta_{Si} = 1 - S,$$

i.e., top Si-atom density in 2×3-Na expressed in ML units is equal to the fraction of surface area between islands. For a Si-atom density evaluation, the STM images of the Si(100)2×3-Na surface in saturation were used. The widest terraces were chosen, and the area adjacent to the step edges was excluded from consideration. During area determination we took into account the existence of surface defects which
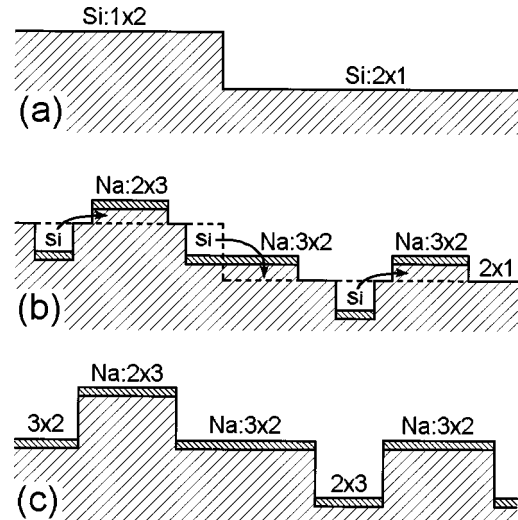

FIG. 3. Schematic illustration of Si(100)2×3-Na phase formation: (a) Si(100)2×1 terraces separated by monoatomic steps prior to Na deposition. (b) Initial stage of Si(100)2×3-Na surface phase formation. Directions of Si mass transport are shown by solid arrows. The location of terraces before Na deposition is shown by the dashed line. (c) Completion of Si(100)2×3-Na surface phase formation.

pin some Si atoms and do not allow them to participate in 2×3-Na phase formation. This estimation results in a value of 0.38 ± 0.08ML which is believed to correspond to $\frac{1}{3}$ ML, i.e., to two Si atoms per 2×3 unit cell.

The obtained data provide a ground for discussion on the Si(100)2×3-Na atomic arrangement. Returning to the questions raised in Sec. I, it can be concluded that the structure of the Si(100)2×3-Na phase should differ significantly from those of Si(100)2×3 reconstructions induced by K, Cs, Ba, and Sr, since the 2×3-Na phase is the only one among other 2×3 phases in which the top Si layer is found to undergo substantial reordering. Thus none of the structural models proposed for Si(100)2×3-K (Cs, Ba, Sr) phases is suitable for the Si(100)2×3-Na phase. The 2×3-Na structure model proposed by Glander and Webb[22] incorporates the Si surface atom reordering, but it is in contradiction with some data of the present work; that is, their model suggests the top Si-atom density to be 2/3 ML (instead of 1/3 ML), and the direction of the $3a$ periodicity to be orthogonal (instead of parallel) to the direction of Si dimers of original Si(100)2×1 surface. These requirements are satisfied in the model shown in Fig. 4. To fit the proper orientation of the 2×3 unit cell, we suggest that the basic Si(100) plane has a structure similar to that of the Si(100)3×1-H[32] surface, i.e., it contains a sequential alternation of Si dimer rows and Si-atom rows. Two additional Si atoms per 2×3 unit cell are supposed to form an extra dimer on top of the Si(100)3×1 surface. Two Na atoms (shown as dark circles in Fig. 4) yield a Na coverage of 1/3 ML, in agreement with the data of Ref. 21.

Some indication on the validity of the proposed atomic geometry can be found in high-resolution STM images of the Si(100)2×3-Na surface (Fig. 5). In filled-state STM images, the 2×3-Na unit cell always shows up as asymmetric with respect to the mirror plane along the $2a$ periodicity direction. However, the appearance of this surface turns out to depend greatly on the tunneling conditions. The most significant
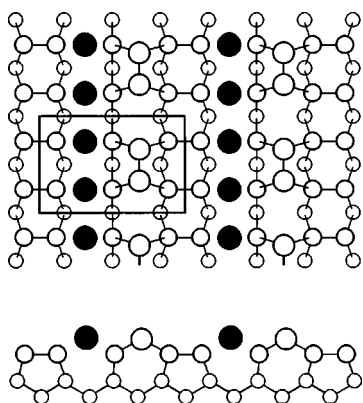
FIG. 4. Structural model for Si(100)2×3-Na surface phase. Silicon atoms are shown as open circles, and sodium atoms are shown as dark circles. The 2×3 unit cell is outlined.

variations in STM images are associated with a variation in tunneling current, while a variation in bias voltage in the range from +1 to +3 V has smaller effect. As an example, Fig. 5 shows the appearance of the same region of the
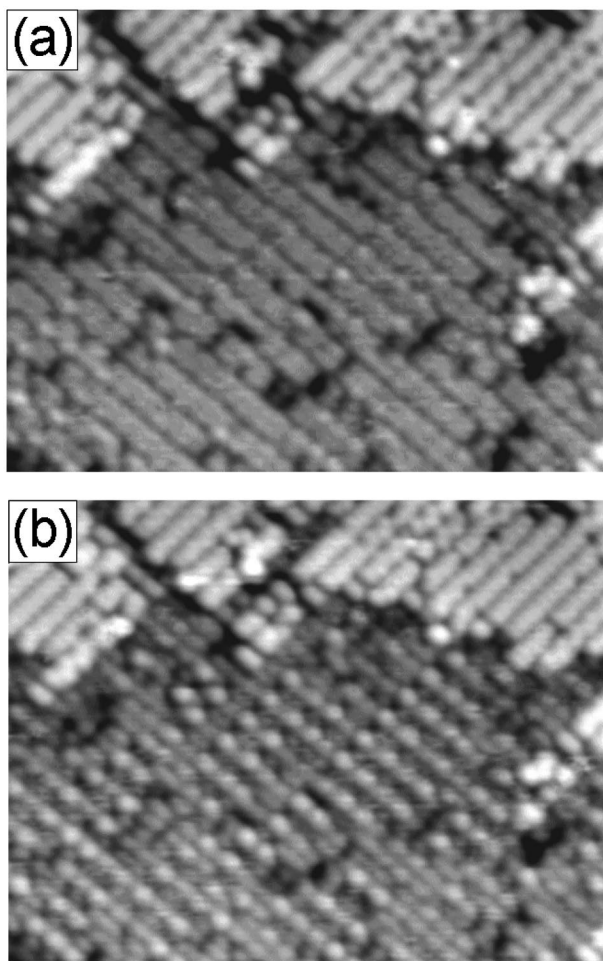

FIG. 5. STM images of the same 250×220-Å^2 area of the Si(100)2×3-Na surface acquired at the same bias voltage of +2 V but at different tunneling currents: (a) at 0.2 nA ("low current" regime) and (b) at 1.7 nA ("high current" regime). The appearance of 2×3-Na changes significantly, while the appearance of Si(100)2×1 surface seen in the upper part of the figures remains practically unchanged.
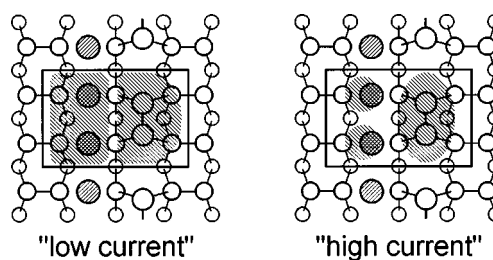

FIG. 6. Location of protrusions seen in STM images with respect to the proposed Si(100)2×3-Na structural model. Silicon atoms are shown as open circles, and Na atoms are shown as shaded circles.

Si(100)2×3-Na surface in STM images acquired in "low current" and "high current" regimes. The transition current value separating "low current" and "high current" ranges varies from one STM tip to another. However, the features characteristic of each acquisition regime were reproducibly obtained with different tips.

This behavior can be explained on the basis of recently reported theoretical results on STM imaging of the Na/Si(100) surface,[31] where it was shown that the vertical position of Na atoms is very sensitive to a tip-induced electric field whose variation is associated with the change of tunneling current rather than that of bias voltage. It was also reported that Si atoms are less sensitive to the field. Taking into account the different response of Na and Si atoms to the applied field, we attempted to find the registry of the model to the STM images. The consideration was based on the assumption that the most significant field-induced variations should occur in the sites of Na-atom location. The results of these considerations are illustrated by Fig. 6, which shows the registry of the model to the protrusions seen in STM images acquired in "low current" and "high current" regimes. In low current STM images, both Na atoms and the Si dimer show up as oval protrusions of slightly different shape but with the same apparent height. In contrast, in high cur-
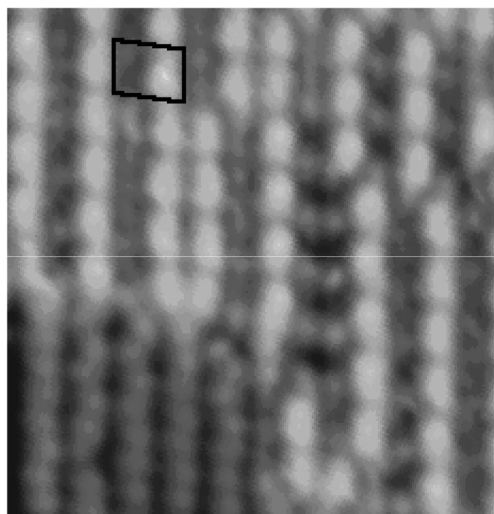

FIG. 7. High-resolution 80×80-Å^2 STM image of a Si(100)2×3-Na surface acquired at a bias voltage of +2 V and a tunneling current of 1 nA. 2×3 unit cell is shown. The region in the lower left part is occupied by the intact Si(100)2×1 surface.

rent STM images, the ''Na subunit'' within the 2×3 unit cell becomes noticeably lower and each Na atom is believed to be resolved (see Fig. 7).

Closer inspection of high-resolution STM images reveals some additional features of the Si(100)2×3-Na structure. The coexistence of a 2×3-Na surface phase with a region of an intact Si(100)2×1 surface (lower left part of Fig. 7) enables us to determine that Na atoms occupy basically the cave sites, in agreement with the recent theoretical results.[31] One can notice that some Na atoms are missing; i.e., some unit cells contain two Na atoms as suggested by the model, while the others have only one atom per unit cell. This is believed to be due to the fact that formation of the 2×3-Na phase takes place at temperatures where Na desorption is already noticeable. The relatively high density of structural defects is also a characteristic feature of the Si(100)2×3-Na surface. For example, one can see two antiphase domain boundaries in Fig. 7, one being immediately below the outlined unit cell and the second two unit cells to the right. In accordance with the proposed structural model, the origin most of the defects is a simple permutation of Na and Si subunits within a 2×3 unit cell.

IV. CONCLUSION

Formation of the Si(100)2×3-Na surface phase at Na deposition onto a Si(100)2×1 surface held at about 400 °C has been studied by scanning tunneling microscopy. Evi-

dence has been found that the growth of the Si(100)2×3-Na phase involves substantial Si mass transport. Si reordering has been found to be due to the fact that the top Si-atom density in Si(100)2×3-Na phase is 1/3 ML. The obtained information on the 2×3-Na structure [Si-atom density, registry of the 2×3 unit cell with respect to original Si(100)2×1 surface, and appearance of the 2×3-Na surface in the STM images] are incorporated into the proposed structural model of the Si(100)2×3-Na surface phase. In the model, the 2×3 unit cell contains two Na atoms in cave sites, and one extra Si dimer residing on a (3×1)-reconstructed surface with a sequential alternation of Si dimer rows and Si-atom rows.

*Author to whom correspondence should be addressed. FAX: +81 6 876 4564. Electronic address: oura@ele.eng.osaka-u.ac.jp

[1] V. G. Lifshits, A. A. Saranin, and A. V. Zotov, *Surface Phases on Silicon* (Wiley, Chichester, 1994), p. 450.

[2] J. E. Northrup, Phys. Rev. Lett. **53**, 683 (1984).

[3] J. Nogami, S. Park, and C. F. Quate, J. Vac. Sci. Technol. B **6**, 1479 (1988).

[4] J. Zegenhagen, J. R. Patel, P. E. Freeland, D. M. Chen, J. A. Golovchenko, P. Bedrossian, and J. E. Northrup, Phys. Rev. B **39**, 1298 (1989).

[5] P. J. Bedrossian, R. D. Meade, K. Mortensen, D. M. Chen, J. A. Golovchenko, and D. Vanderbilt, Phys. Rev. Lett. **63**, 1257 (1989).

[6] T. Abukawa, C. Y. Park, and S. Kono, Surf. Sci. **201**, L513 (1988).

[7] C. Y. Park, T. Abukawa, K. Higashiyama, and S. Kono, Jpn. J. Appl. Phys., Part 2 **26**, L1335 (1987).

[8] T. Takahashi, K. Izumi, T. Ishikawa, and S. Kikuta, Surf. Sci. **183**, L302 (1987).

[9] M. Katayama, R. S. Williams, M. Kato, E. Nomura, and M. Aono, Phys. Rev. Lett. **66**, 2762 (1991).

[10] S. Mizuno and A. Ichimiya, Appl. Surf. Sci. **33/34**, 38 (1988).

[11] H. Daimon and S. Ino, Surf. Sci. **164**, 320 (1985).

[12] D. Jeon, T. Hashizume, T. Sakurai, and R. F. Willis, Phys. Rev. Lett. **69**, 1419 (1992).

[13] W. C. Fan and A. Ignatiev, Phys. Rev. B **41**, 3592 (1990).

[14] K. J. Wan, X. F. Lin, and J. Nogami, Phys. Rev. B **46**, 13 635 (1992).

[15] K. Sakamoto, T. Okuda, H. Nishimoto, H. Daimon, S. Suga, T. Kinoshita, and A. Kakizaki, Phys. Rev. B **50**, 1725 (1994).

[16] H. H. Weitering, N. J. DiNardo, R. Pérez-Sandoz, J. Chen, and E. J. Mele, Phys. Rev. B **49**, 16 837 (1994).

[17] S. C. Erwin, Phys. Rev. Lett. **75**, 1973 (1995).

[18] H. H. Weitering, X. Shi, and S. C. Erwin, Phys. Rev. B **54**, 10 585 (1996).

[19] Y. Enta, T. Kinoshita, S. Suzuki, and S. Kono, Phys. Rev. B **36**, 9801 (1987).

[20] A. Brodde, Th. Bertrams, and H. Neddermeyer, Phys. Rev. B **47**, 4508 (1993).

[21] G. S. Glander and M. B. Webb, Surf. Sci. **222**, 64 (1989).

[22] G. S. Glander and M. B. Webb, Surf. Sci. **224**, 60 (1989).

[23] R. Holtom and P. M. Gundry, Surf. Sci. **63**, 263 (1977).

[24] T. Abukawa, T. Okane, and S. Kono, Surf. Sci. **256**, 370 (1991).

[25] H. Xu, H. Hashizume, and T. Sakurai, Phys. Status Solidi A **151**, 329 (1995).

[26] W. C. Fan and A. Ignatiev, Surf. Sci. **253**, 297 (1991).

[27] T. Urano, K. Tamiya, K. Ojima, S. Hongo, and T. Kanaji, Surf. Sci. **357/358**, 459 (1996).

[28] W. C. Fan, N. J. Wu, and A. Ignatiev, Phys. Rev. B **42**, 1254 (1990).

[29] R. Z. Bakhtizin, J. Kishimoto, T. Hashizume, and T. Sakurai, Appl. Surf. Sci. **94/95**, 478 (1996).

[30] R. Z. Bakhtizin, J. Kishimoto, T. Hashizume, and T. Sakurai, J. Vac. Sci. Technol. B **14**, 1000 (1996).

[31] A. Pomyalov and Y. Manassen, Surf. Sci. **382**, 275 (1997).

[32] Y. J. Chabal and K. Raghavachari, Phys. Rev. Lett. **54**, 1055 (1985).